Stem Cell Reports

Article

ISSCR

OPEN ACCESS

Generation of Scaffoldless Hyaline Cartilaginous Tissue from Human iPSCs

Akihiro Yamashita,[1] Miho Morioka,[1] Yasuhito Yahara,[1] Minoru Okada,[1] Tomohito Kobayashi,[1,2] Shinichi Kuriyama,[2] Shuichi Matsuda,[2] and Noriyuki Tsumaki[1,3,*]

[1]Cell Induction and Regulation Field, Department of Cell Growth and Differentiation, Center for iPS Cell Research and Application, Kyoto University, Kyoto 606-8507, Japan
[2]Department of Orthopaedic Surgery, Graduate School of Medicine, Kyoto University, Kyoto 606-8507, Japan
[3]Japan Science and Technology Agency, CREST, Tokyo 102-0075, Japan
*Correspondence: ntsumaki@cira.kyoto-u.ac.jp
http://dx.doi.org/10.1016/j.stemcr.2015.01.016

SUMMARY

Defects in articular cartilage ultimately result in loss of joint function. Repairing cartilage defects requires cell sources. We developed an approach to generate scaffoldless hyaline cartilage from human induced pluripotent stem cells (hiPSCs). We initially generated an hiPSC line that specifically expressed GFP in cartilage when teratoma was formed. We optimized the culture conditions and found BMP2, transforming growth factor β1 (TGF-β1), and GDF5 critical for GFP expression and thus chondrogenic differentiation of the hiPSCs. The subsequent use of scaffoldless suspension culture contributed to purification, producing homogenous cartilaginous particles. Subcutaneous transplantation of the hiPSC-derived particles generated hyaline cartilage that expressed type II collagen, but not type I collagen, in immunodeficiency mice. Transplantation of the particles into joint surface defects in immunodeficiency rats and immuno-suppressed mini-pigs indicated that neocartilage survived and had potential for integration into native cartilage. The immunodeficiency mice and rats suffered from neither tumors nor ectopic tissue formation. The hiPSC-derived cartilaginous particles constitute a viable cell source for regenerating cartilage defects.

INTRODUCTION

Articular cartilage covers the ends of bones and provides shock absorption and lubrication to diarthrodial joints. Articular cartilage is a highly specialized tissue composed of chondrocytes and a specific extracellular matrix (ECM) that consists of types II, IX, and XI collagen and proteoglycans, but not type I collagen. Such cartilage is called hyaline cartilage. Focal defects or degeneration of articular cartilage due to trauma or regional necrosis can progressively degenerate large areas of cartilage owing to a lack of repair capacity. These conditions ultimately result in a loss of joint function, inducing osteoarthritis. Autologous chondrocyte transplantation is a successful cell therapy for repairing focal defects of articular cartilage. However, this approach suffers from the need to sacrifice healthy cartilage for biopsies and the formation of fibrocartilaginous repair tissue containing type I collagen (Roberts et al., 2009), because the required in vitro expansion induces the dedifferentiation of chondrocytes toward fibroblastic cells. In addition, it is difficult to achieve the integration of repair tissue into the adjacent native cartilage. Other attractive cell sources for repairing cartilage defects include mesenchymal stem cells (MSCs). However, MSCs can differentiate into multiple cell types, resulting in a mixture of cartilaginous tissue, fibrous tissue (as indicated by the expression of type I collagen), and hypertrophic tissue (as indicated by the expression of type X collagen) (Mithoefer et al., 2009; Steck et al., 2009). Despite the ability to achieve short-term clinical success, non-hya-

line repair tissue is eventually lost, because it does not possess the proper mechanical qualities.

Currently, a new option for repairing defects in cartilage has become available by applying human induced pluripotent stem cells (hiPSCs) with self-renewal and pluripotent capacities without ethical issues. It has been reported that both human embryonic stem cells (hESCs) and hiPSCs can be differentiated into chondrogenic lineages (Barberi et al., 2005; Vats et al., 2006; Koay et al., 2007; Hwang et al., 2008; Bigdeli et al., 2009; Nakagawa et al., 2009; Bai et al., 2010; Oldershaw et al., 2010; Toh et al., 2010; Medvedev et al., 2011; Umeda et al., 2012; Wei et al., 2012; Koyama et al., 2013; Cheng et al., 2014; Ko et al., 2014; Zhao et al., 2014). However, the purity and homogeneity of the resultant cartilage vary, and in vivo transplantation studies have not investigated the risk of teratoma formation systematically. The transplantation of inappropriately differentiated embryonic stem cells (ESCs) results in teratoma formation and tissue destruction at implanted sites, as shown in experiments using murine ESCs (Wakitani et al., 2003; Taiani et al., 2010). The transplantation of hiPSC-derived cells also carries the risk of tumor formation in association with the artificial reprogramming process (Okita et al., 2007; Yamashita et al., 2013). Therefore, an optimized protocol for driving hiPSC differentiation toward chondrocytes that generates pure cartilage without tumor formation in vivo is needed. In this study, we aimed to generate hiPSC-derived cartilage that exhibits the ability to (1) generate pure cartilage in vivo, (2) integrate neocartilage into the adjacent native articular cartilage, and (3)
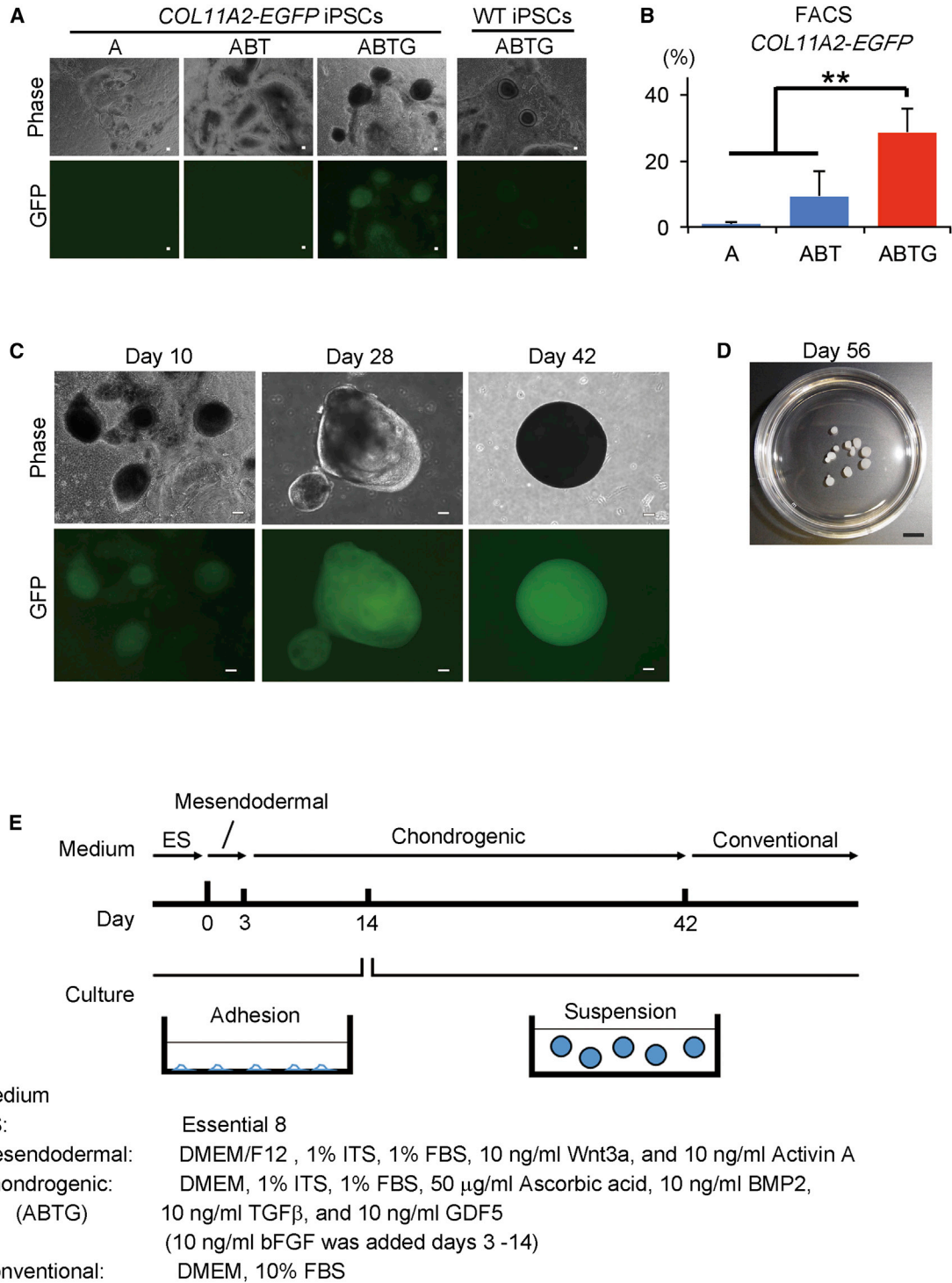
Figure 1. Optimized Protocol for Differentiating hiPSCs toward Chondrocytes

(A) Images of hiPSC-derived cells induced in the presence of the indicated supplement on day 14. Top panels: phase view. Bottom panels: GFP fluorescence view. The right panels show images of cells derived from hiPSCs that did not bear the *COL11A2-EGFP* transgene cultured in the presence of ABTG supplementation. Scale bars, 50 μm.

(B) FACS analysis of *COL11A2-EGFP*-positive cells in the iPSC-derived cell culture in the presence of the indicated supplements on day 14. The error bars denote the means ± SD of three individual experiments. $**p < 0.01$.

(legend continued on next page)

produce neither tumors nor ectopic tissue formation when transplanted in immunodeficiency animals. We therefore developed a chondrogenic differentiation method by taking advantage of real-time monitoring of the chondrocytic phenotype of cells derived from *COL11A2-EGFP* hiPSCs. We then examined whether the resultant hiPSC-derived cartilage met the above specifications using an animal transplantation model.

RESULTS

Establishment of an Efficient Chondrogenic Differentiation Method Using *COL11A2-EGFP* Reporter hiPSCs

In order to design a method for the chondrogenic differentiation of hiPSCs, we first attempted to create chondrocyte-specific reporter hiPSC lines. Because the α2(XI) collagen chain gene (*COL11A2*) is expressed in a chondrocyte-specific manner, we introduced the human *COL11A2-EGFP* transgene, where *EGFP* cDNA was linked to the *COL11A2* promoter and enhancer sequences (Figure S1A), into the 409B2 hiPSC line using the piggyBac vector system and established stable cell lines. To examine the expression pattern of the transgene, we transplanted the *COL11A2-EGFP* hiPSC lines into severe combined immunodeficiency (SCID) mice, which formed teratomas. GFP was exclusively expressed in the chondrocytes of cartilage in the teratomas (Figure S1B), indicating that *COL11A2-EGFP* hiPSCs express GFP only when they differentiate into chondrocytes. We used these *COL11A2-EGFP* hiPSCs in order to search for the culture condition that drives the differentiation of hiPSCs toward chondrocytes.

The *COL11A2-EGFP* hiPSCs were initially differentiated into mesendodermal cells by Wnt3a and Activin A, as previously reported (Oldershaw et al., 2010; Umeda et al., 2012), for 3 days. On day 3, the medium was changed to basal medium supplemented with chondrogenic factors aimed to commit the cells to the chondrocytic lineage. We tested three types of supplementation: A (ascorbic acid), ABT (ascorbic acid, BMP2, and transforming growth factor β1 [TGF-β1]), and ABTG (ascorbic acid, BMP2, TGF-β1, and GDF5). These supplements were added to the basal medium (DMEM with 1% insulin-transferrin-selenium [ITS] and 1% fetal bovine serum [FBS]). Basic fibroblast growth factor (bFGF) was added during the adherent culture (day 3 to day 14) to promote cell proliferation. The hiPSC-derived mesendodermal cells did not form nodules

under the conditions of A supplementation, whereas they became focally multilayered and formed nodules under the conditions of ABT or ABTG supplementation on day 14 (Figure 1A). The nodules observed under the conditions of ABTG supplementation specifically exhibited *COL11A2-EGFP* fluorescence, whereas the nodules formed under the conditions of ABT supplementation did not. Additionally, ABTG produced a significantly higher ratio of *COL11A2-EGFP*-positive cells than did either A or ATB according to fluorescence-activated cell sorting (FACS) analysis (Figure 1B). The characteristics of human *COL11A2-EGFP*-positive cells on day 14 may corresponded to those of early precursor cells and chondrocyte-committed cells, as the *Col11a2-LacZ* (Tsumaki et al., 1996) and *Col11a2-EGFP* (Hiramatsu et al., 2011) reporter genes were expressed in condensing mesenchymal cells in the limb buds of transgenic mice at 12.5 days postcoitum.

In order to generate scaffold-free cartilaginous tissue from hiPSC-derived chondrogenically committed cells in vitro, we considered transferring the cells into a three-dimensional culture, such as a suspension culture or pellet culture. Because the cell nodules cultured in ABTG supplementation were readily detached, likely due to the low adherent properties of cartilaginous ECM, we chose a suspension culture as a three-dimensional culture. The nodules suspended in medium formed particles, which showed a gradual increase in GFP fluorescence (Figure 1C) and white cartilaginous appearance (Figure 1D). Through these examinations, we established the differentiation protocol shown in Figure 1E. Here, the hiPSCs were initially differentiated into mesendodermal cells by Wnt3a and Activin A for 3 days. On day 3, the medium was changed to chondrogenic medium (ABTG supplementation) to commit the cells to the chondrocytic lineage. The cell nodules were then subjected to the suspension culture on day 14.

The effectiveness of ABTG supplementation in inducing chondrogenic differentiation was confirmed by the presence of high expression levels of chondrocyte-marker genes in the particles on day 28 (Figure S1C) and the intense staining of the particles with safranin O on day 42 (Figure S1D). These results suggest the promise of our protocol for differentiating hiPSCs toward chondrocytes.

In order to examine whether BMP2 and/or TGF-β1 are dispensable for chondrogenic differentiation, we also tested the effects of ABG (ascorbic acid, BMP2, and GDF5) and ATG (ascorbic acid, TGF-β1, and GDF5) supplementation. ABG and ATG produced smaller proportions of *COL11A2-EGFP*-positive cells than did ABTG on day 14
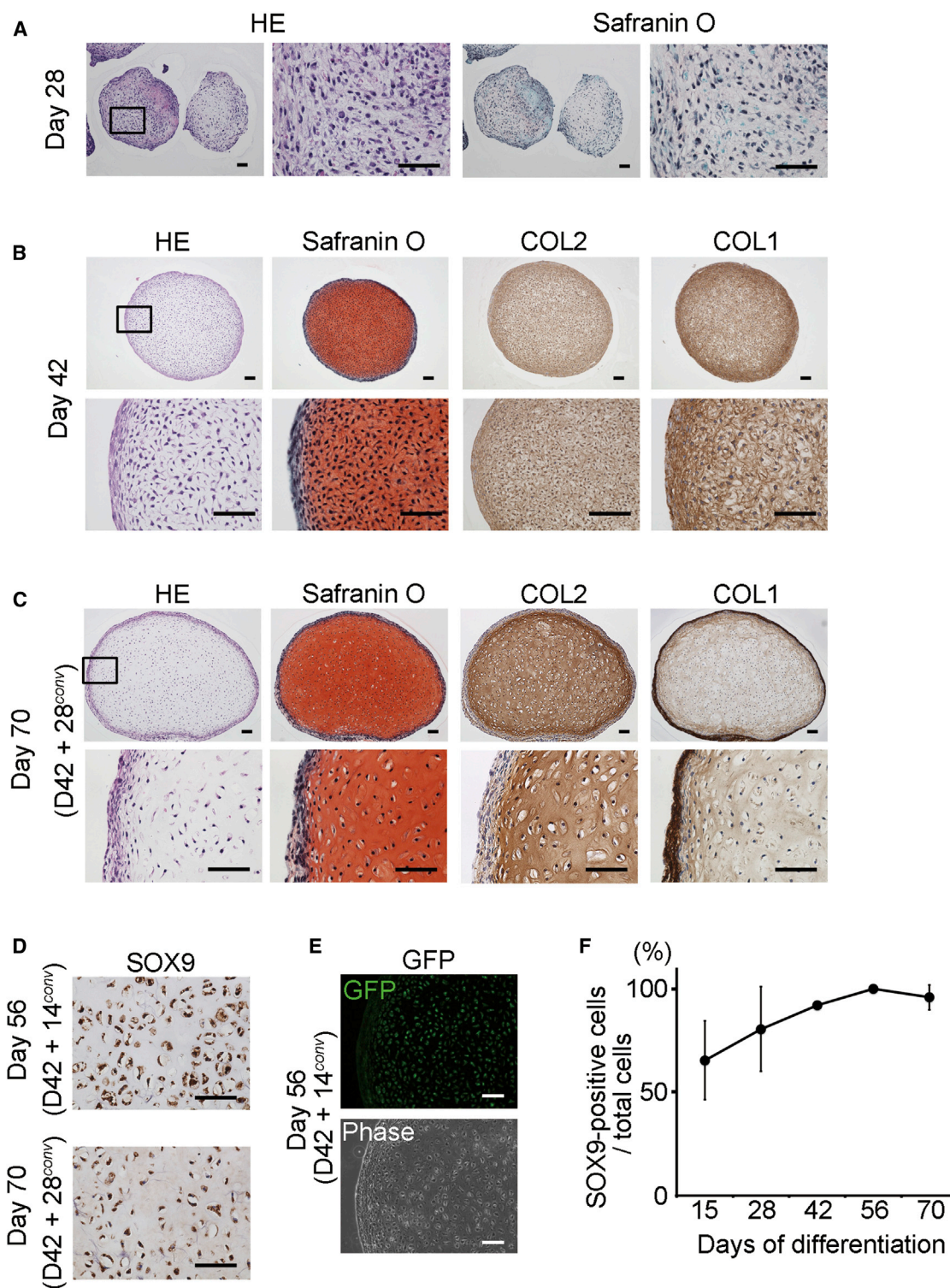
(C) Phase and GFP fluorescence images of the *COL11A2-EGFP* hiPSC-derived cell culture under ABTG supplementation. Scale bars, 50 μm.
(D) Images of the hiPSC-derived particles on day 56 in 3.5-cm dishes. Scale bar, 5 mm.
(E) Schematic representation of the protocol for differentiating hiPSCs toward chondrocytes.
See also Figure S1.

Figure 2. Histological Analysis of hiPSC-Derived Particles in Suspension Culture

Semiserial sections were stained with H&E and safranin O-fast green-iron hematoxylin and immunostained with anti-type II collagen antibodies, anti-type I collagen antibodies, anti-SOX9 antibodies, and anti-GFP antibodies, as indicated. Scale bars, 50 μm.

(A) A particle 28 days after the start of differentiation of hiPSCs (day 28). The second and fourth panels are magnifications of the boxed region.

(legend continued on next page)

(Figure S1E). Particles induced under the conditions of ABG and ATG supplementation on day 42 did not contain cartilaginous elements (Figure S1F). These results collectively suggest that BMP2, TGF-β1, and GDF5 are all necessary for the chondrogenic differentiation of hiPSCs in our protocol. Therefore, we employed ABTG supplementation for the chondrogenic differentiation of hiPSCs. Hereafter, chondrogenic medium corresponds to medium supplemented with ABTG. We used this differentiation method in a recently published paper for hiPSC disease modeling (Yamashita et al., 2014).

Cartilaginous Tissues Were Formed from Multiple Independent hiPSC Lines

A histological analysis of the particles performed on day 42 showed that cartilaginous tissues could also be generated from other hiPSC lines, including 604B1, HDF-11, and KF4009-1 (Figure S2A). The 409B2, HDF-11, and KF4009-1 lines were induced from dermal fibroblasts obtained from different individuals, and the 604B1 line was induced from the blood cells obtained from a different individual. All hiPSC lines were generated using episomal vectors. These results suggest that cartilaginous tissues were formed from multiple independent hiPSC lines by our protocol.

Hyaline-Cartilaginous Maturation of Particles in Suspension Culture

We performed histological analysis of the particles over time. The particles consisted of cells embedded in a small amount of ECM stained slightly with safranin O on day 28 (Figure 2A). The ECM in the particles matured, as indicated by intense staining with safranin O on day 42 (Figure 2B). Immunohistochemistry results showed that the ECM contained both type I and type II collagen. When we continued to culture the particles in chondrogenic medium, they maintained an expression of type I collagen on day 70 (Figure S2B) and day 140 (Figure S2C).

To reduce type I collagen expression and achieve hyaline cartilage maturation, we further manipulated the culture condition. We replaced chondrogenic medium with conventional medium (DMEM + 10% FBS) on day 14, 28, or 42 and continued the cultures for another 28 days. Medium replacement on day 42 resulted in the formation of intensely safranin-O-positive cartilaginous ECM with increased type II collagen expression and decreased type I collagen expression (Figure 2C). Medium replacement on day 14 (Figure S2D) or 28 (Figure S2E) resulted in continued expression of type I collagen. We confirmed the recapitulation of the decrease of type I collagen expression by replacing the chondrogenic medium with conventional medium on day 42 in another iPSC line, 604B1 (Figures S2F and S2G). We additionally found that replacing chondrogenic medium with medium supplemented with A, ABT, ABG, or ATG also decreased type I collagen expression (Figure S2H). These results suggest that ABTG is necessary for the commitment to chondrocytic lineage but is not continuously necessary. The three-dimensional structure of the particles formed by day 42 was sufficient and effective at inducing the hyaline-cartilaginous maturation of chondrocytes.

The particles were surrounded by a membranous structure that expressed type I collagen (Figures 2B and 2C). This membrane probably corresponded to the perichondrium, which is formed during development. The ratio of SOX9-positive cells in the particles, except for those in the surface membrane, gradually increased, reaching 91.8% ± 0.91% on day 42 and almost 99.7% ± 0.2% on day 56 (Figures 2D and 2F). Almost all cells expressed COL11A2-EGFP on day 56 (Figure 2E). Type X collagen expression was undetectable (Figure S2I).

Suspension Culture Facilitates the Chondrogenic Differentiation of iPSCs and Elimination of Non-chondrocytic Cells

We examined how the transfer of the cell nodules to the suspension culture affects chondrogenic differentiation. When we maintained the cell nodules in the adhesion culture beyond day 14, the nodules poorly formed cartilaginous tissue on day 42 (Figure S3A), which contrasts the cartilaginous appearance of the particles cultured in suspension on day 42 (Figure 2B). These results suggest that the suspension culture facilitates the cartilaginous maturation of iPSC-derived chondrogenic cells.

After transferring the particles to suspension culture in new dishes, the dish bottoms gradually became covered with cells, suggesting that some of the cells detached

(B) A particle on day 42. Bottom panels are magnifications of the boxed region.

(C) A particle on day 70. The medium was switched from chondrogenic medium to conventional medium on day 42. Bottom panels are magnifications of the boxed region.

(D) Histological sections of particles obtained on days 56 and 70 were immunostained with anti-SOX9 antibodies.

(E) Histological sections of particles obtained on day 56 were immunostained with anti-GFP antibodies.

(F) The ratio of the number of SOX9-positive cells per total cells during the maturation of particles. Cells were counterstained with hematoxylin. The numbers of cells in the particles, except for the surface layers, were counted. n = 3 particles. The error bars denote the means ± SD.

See also Figures S2 and S3 and Table S1.
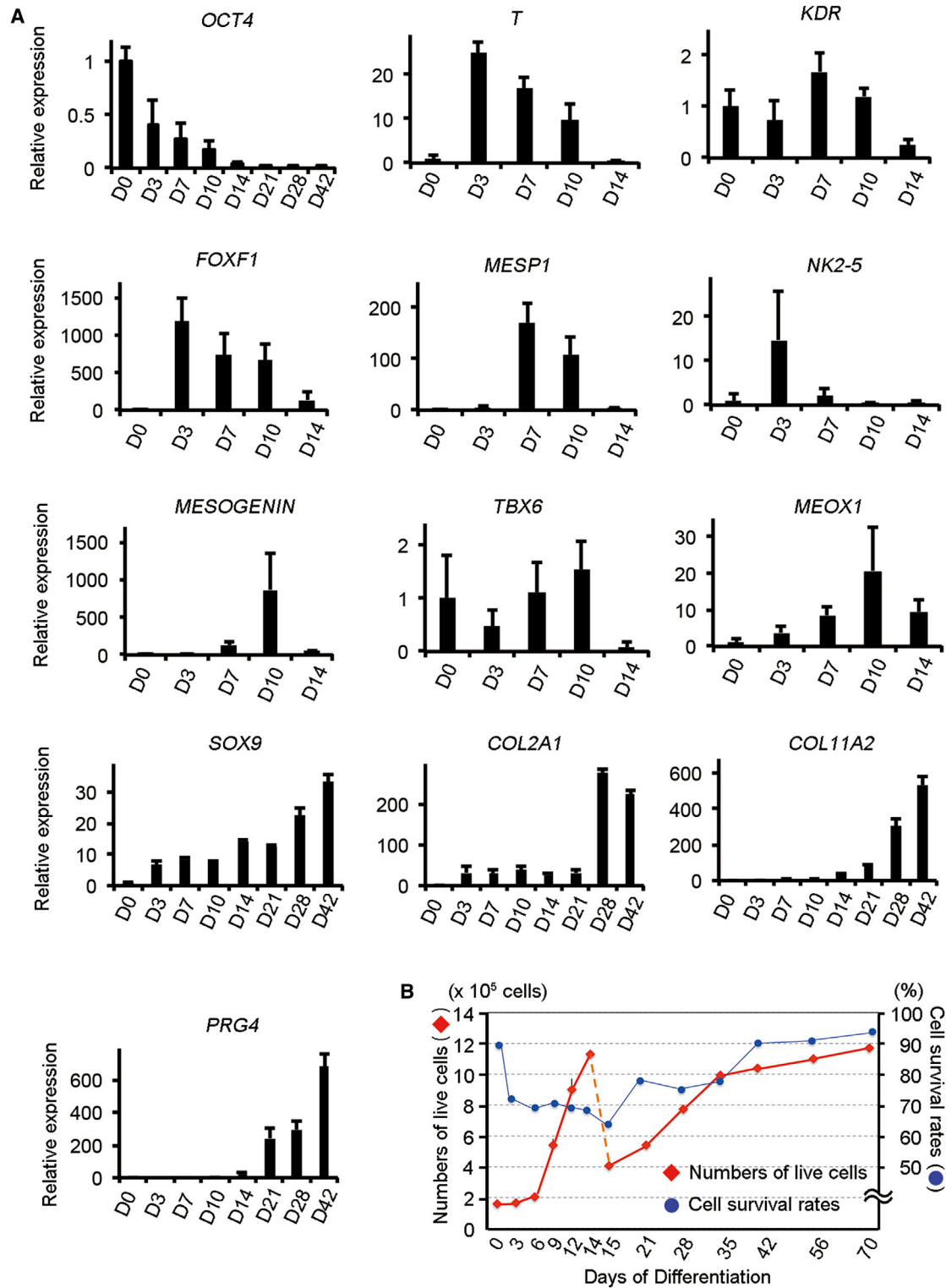
Figure 3. Analysis of Marker Gene Expression and Growth and Death of hiPSC-Derived Cells during Differentiation

We collected whole cells during the adhesion culture until day 14. From day 15, we collected only particles, not cells attached to the bottom of the dishes.

(legend continued on next page)

from the particles, attached to the dish bottoms, and proliferated. These cells had a spindle-shaped morphology and did not exhibit *COL11A2-EGFP* fluorescence (Figure S3B). The expression analysis showed that the cells in the suspended particles expressed much higher levels of chondrocyte marker genes than the cells attached to the dish bottom (Figure S3C). These results suggest that non-chondrocytic cells were removed from the particles during the suspension culture, thus enhancing the cartilage purity.

Sequential Analysis of the Growth and Differentiation of Chondrogenically Differentiating hiPSCs

At the start of the differentiation of hiPSCs, the addition of Wnt3a and Activin A with a low concentration of FBS (1%) decreased the expression of pluripotent markers and transiently increased the expression of an early mesendoderm marker (*BRACHYURY*, also known as *T*) on day 3 (Figures 3A and S4), as previously reported (Oldershaw et al., 2010). The lack of increase in the number of cells despite cell division and the reduced cell survival observed on day 3 (Figure 3B) suggest that the non-mesendoderm cells preferentially died under these conditions, contributing to the formation of a mesendodermal-cell-rich population. We suggest that the low concentration of FBS was insufficient for the survival of non-mesendodermal cells, whereas mesendodermal chondrocytes could survive due to the presence of essential cytokines. After switching the medium to chondrogenic medium on day 3, the expression of pluripotent markers further decreased from days 7 through 14, while the expression levels of many of the mesodermal markers increased (Figures 3A and S4), suggesting that the hiPSC-derived cells produced according to this protocol included a mixture of both paraxial mesodermal cells and lateral plate mesodermal cells. The number of cells increased until day 14 (Figure 3B), reflecting the formation of nodules (multilayered cells).

On day 14, we detached the cell nodules from the dish bottoms to form particles and transferred them to a suspension culture. We counted only the number of cells in the particles, not the number of monolayer cells that were left attached to the dishes (Figure 3B). The number of cells in the particles increased slowly and gradually. A certain population of cells continued to die in the particles until day 42. At the end of the culture, the number of cells in all particles was approximately seven times the number of hiPSCs observed at the start of differentiation (Figure 3B). On average, we began the differentiation procedure with $1.6 \pm 0.1 \times 10^5$ hiPSCs per 35-mm dish. The number of cells reached $11.3 \pm 0.3 \times 10^5$ on day 14. Among these cells, $4.06 \pm 0.04 \times 10^5$ participated in the formation of particles. The number of cells in the particles increased to $10.4 \pm 0.2 \times 10^5$ cells on day 42. The number of particles was 14.6 ± 4.0 per dish, and the average diameter of the particles was 0.7 ± 0.2 mm on day 21, 0.8 ± 0.2 mm on day 28, 1.1 ± 0.2 mm on day 42, and 1.4 ± 0.5 mm on day 70.

Chondrocyte hypertrophy appeared to be limited in the particles, as the expression levels of *IHH* and *COL10A1* mRNAs in the particles were lower than that observed in the articular cartilage (Figure S4), and the amount of type X collagen in the particles was undetectable in an immunohistochemical analysis (Figure S2I). Few *COL1A1* mRNAs and some *COL1A2* mRNAs were expressed in the particles (Figure S4). The expression of *OSTEOCALCIN* was absent, suggesting that osteoblastic differentiation did not occur.
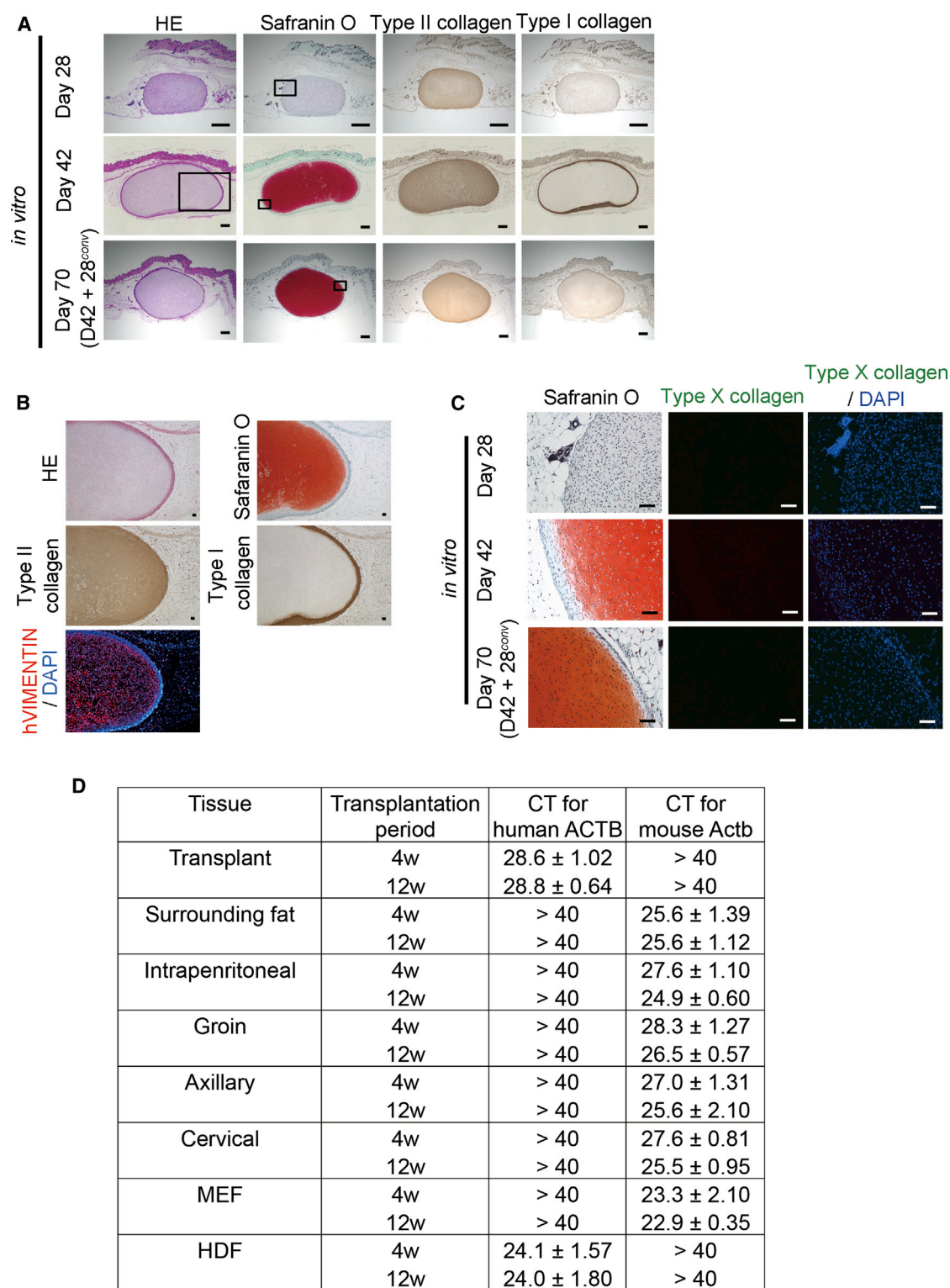
We then performed cellular analysis during differentiation. Differentiation into mesodermal cells appeared around day 10 (Figures 3 and S4). FACS analysis revealed that *COL11A2-EGFP* fluorescence on day 10 was slightly increased compared with that on day 0 (Figure S5A). We divided cells on day 10 into two groups based on the FACS analysis: a GFP (−) cell group, which showed lower GFP fluorescence intensity than the median, and a GFP (+) cell group, which showed higher GFP fluorescence intensity than the median. We isolated both cell groups, cultured them in micromass in chondrogenic medium for a further 10 days, and subjected them to FACS analysis and expression analysis. The GFP (+) cell progeny contained more *COL11A2-EGFP*-positive cells (Figure S5B) and expressed higher expressions of chondrocyte-marker genes (Figure S5C) than the GFP (−) cell progeny. We further confirmed that micromass culture of the GFP (+) cell progeny formed cartilaginous nodules, as indicated by staining with safranin O (Figure S5D). These results suggest that our differentiation method could create a chondrogenic progenitor population (GFP [+] cells) and is efficient at chondrogenic maturation of the progenitor cells.

(A) Real-time RT-PCR expression analysis of marker genes for pluripotency and the development of the mesoderm, chondrocytes, fibroblasts, and osteoblasts. RNA expression levels were normalized to the level of *β-ACTIN* (*ACTB*) expression. n = 3 technical replicates. The data are representative of two independent experiments.

(B) Growth and death of hiPSC-derived cells. The collected cells were subjected to collagenase digestion to obtain a single-cell suspension. Cell numbers were counted after the addition of trypan blue. Cells that did not incorporate trypan blue were considered alive. Cell survival rates indicate the number of live cells divided by the total number of cells. n = 3 dishes.

The error bars denote the means ± SD.

See also Figures S4 and S5 and Tables S2 and S3.

Tissue	Transplantation period	CT for human ACTB	CT for mouse Actb
Transplant	4w	28.6 ± 1.02	> 40
	12w	28.8 ± 0.64	> 40
Surrounding fat	4w	> 40	25.6 ± 1.39
	12w	> 40	25.6 ± 1.12
Intrapenritoneal	4w	> 40	27.6 ± 1.10
	12w	> 40	24.9 ± 0.60
Groin	4w	> 40	28.3 ± 1.27
	12w	> 40	26.5 ± 0.57
Axillary	4w	> 40	27.0 ± 1.31
	12w	> 40	25.6 ± 2.10
Cervical	4w	> 40	27.6 ± 0.81
	12w	> 40	25.5 ± 0.95
MEF	4w	> 40	23.3 ± 2.10
	12w	> 40	22.9 ± 0.35
HDF	4w	24.1 ± 1.57	> 40
	12w	24.0 ± 1.80	> 40

Figure 4. Transplantation of hiPSC-Derived Particles on Day 28, 42, or 70 into the Subcutaneous Spaces of SCID Mice
Mice were sacrificed 12 weeks after transplantation. Histological analysis of the transplanted sites was performed.
(A) Semiserial sections were stained with H&E and safranin O-fast green-iron hematoxylin and immunostained with anti-type II and anti-type I collagen antibodies. Scale bars, 500 μm.

(legend continued on next page)

In Vivo Pure Cartilage Formation Induced by hiPSC-Derived Cartilage without Tumor Formation or Ectopic Tissue Formation in SCID Mice

To assess the chondrogenic activity of the hiPSC-derived cartilage in vivo, we transplanted the cells into the subcutaneous spaces of SCID mice. We transplanted hiPSC-derived chondrocyte particles on day 28, 42, or 70 (chondrogenic medium was replaced with conventional medium on day 42) and sacrificed the mice 12 weeks after transplantation. A histological analysis revealed the formation of cartilaginous tissues in two out of six transplantation sites for day-28 particles, four out of six for day-42 particles, and two out of six for day-70 particles. Transplantation of day-42 particles resulted in the formation of the most hyaline-like cartilage, as indicated by intense safranin O staining, high type II collagen expression, low type I collagen expression (Figures 4A and 4B), and low type X collagen expression (Figure 4C). Transplantation of day-28 particles showed weak safranin O staining. The hyaline cartilaginous tissue generated by the transplantation of particles on day 42 was surrounded by a membrane that expressed type I collagen. Immunohistochemistry using anti-human vimentin antibodies showed that the cells in the hyaline cartilage were hiPSC derived, whereas the cells in the surrounding membrane were derived from the mice (Figure 4B). There were no signs of teratoma or other tumor formation in any of the transplanted sites. These results suggest that hiPSC-derived cartilage has the ability to form and maintain hyaline cartilage in vivo for 12 weeks.

We next examined whether the transplanted cells induce ectopic tissue formation. The human β-actin sequence was not amplified within the range of 40 cycles in real-time RT-PCR reactions among either the organs or lymph nodes of SCID mice 4 and 12 weeks after transplanting particles on day 42 (Figure 4D). Our control experiment showed that this assay can be used to detect human sequences at a Ct (cycle threshold) value of 40 among samples containing 0.0003% human cells (Figure S6A). These results suggest that hiPSC-derived chondrocyte particles on day 42 form neither tumors nor ectopic tissue lesions when transplanted in vivo.

For long-term observation, we sacrificed the mice 12 months after transplanting hiPSC-derived particles on day 42, harvested the transplanted sites, and subjected them to histological analysis. All six samples showed cartilage hypertrophy, as indicated by the expression of type X collagen (Figure 5). Among these samples, five had portions of the cartilage replaced with bone-like tissue, but a substantial amount of cartilage with a morphology resembling epiphyseal cartilage remained. These results suggest that the hiPSC-derived cells produced using our protocol undergo hypertrophy, although at a very slow rate. There were no signs of teratoma or other tumor formation at any of the transplanted sites.

In order to obtain insight into why the hiPSC-derived cartilage in the subcutaneous space of SCID mice was stable, we transplanted chondrogenically differentiated MSC pellets (Takara, PT-2501) without a scaffold into the subcutaneous space of SCID mice as a control. No cells survived 4 weeks after transplantation (n = 6). It is difficult, however, to directly compare the results from the transplantation of hiPSC-derived cartilaginous particles with those from the transplantation of MSC-derived cartilaginous pellets, because the two cell types had reached different stages and their route to chondrogenesis may be different. Nevertheless, this result is consistent with the notion that the immunosuppressed environment induced by il2rg mutation (SCID) is not the only factor associated with the long-term preservation of cartilage. Rather, the presence of a cartilaginous tissue structure composed of chondrocytes embedded in the extracellular matrix in the particles may be another factor required for cartilage preservation.

hiPSC-Derived Cartilaginous Particles Can Be Orthotopically Transplanted without Any Tumor Formation or Ectopic Tissue Formation in SCID Rats

We transplanted hiPSC-derived cartilaginous particles into defects created in the articular cartilage of SCID rats. Due to the small size and limited depth of the rat cartilage, we were unable to fix mature particles that were lubricious in their defects. Therefore, we transplanted premature-hiPSC-derived cartilaginous particles obtained on day 28. The defects were filled with hiPSC-derived cells in three of four knees at 1 week and three of four knees at 4 weeks after transplantation, as indicated by the expression of human vimentin (Figure 6A). The day-28 particles produced tissue that exhibited metachromatic staining with toluidine blue

---

(B) Magnified images of day-42 particle progeny in the boxed regions of (A). Semiserial sections were immunostained with anti-vimentin antibodies that recognize only human vimentin. The blue color reflects DAPI. Scale bars, 50 μm.

(C) Magnified images of day-28, 42, and 70 progenies stained with safranin O in the boxed regions of (A). Semiserial sections were immunostained with anti-type X collagen antibody. The blue color reflects DAPI. Scale bars, 50 μm.

(D) RNAs were extracted from various organs of SCID mice that received hiPSC-derived particles on day 42 and subjected to real-time RT-PCR to amplify human and murine β-actin mRNAs. n = 3 mice. The error bars denote the means ± SD. Transplant, transplanted site; Surrounding fat, fat tissue surrounding the transplanted site; Intraperitoneal, intraperitoneal tissue; Groin, groin lymph nodes; Axillary, axillary lymph nodes; Cervical, cervical lymph nodes; MEF, murine embryonic fibroblasts; HDF, human dermal fibroblasts.

See also Figure S6 and Tables S1–S3.
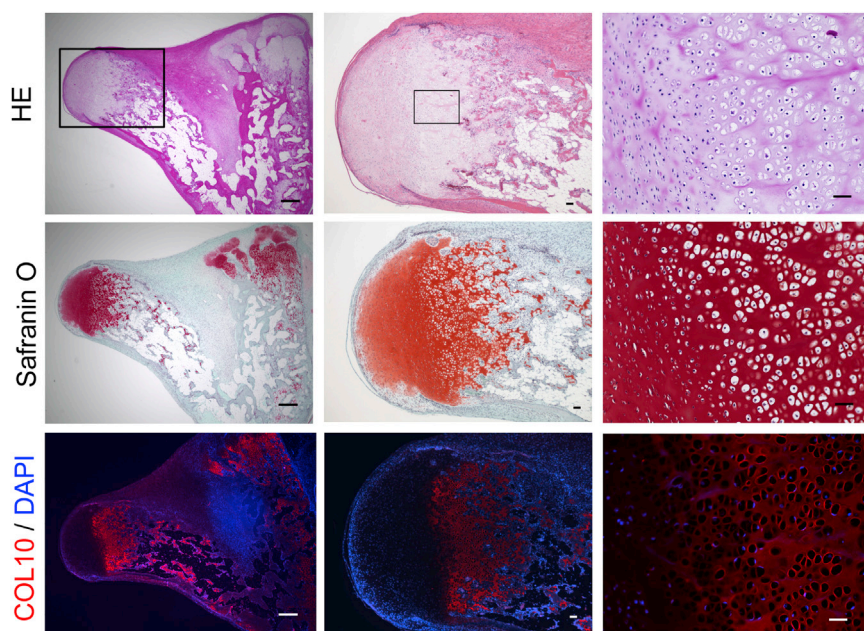
Figure 5. Long-Term Observations of hiPSC-Derived Particles on Day 42 Transplanted into the Subcutaneous Space of SCID Mice

Mice were sacrificed 12 months after transplantation. Semiserial sections were stained with H&E and safranin O-fast green-iron hematoxylin and immunostained with anti-type X collagen antibodies. Magnified images of the boxed regions are shown in panels to the immediate right. Scale bar, 500 μm (left) and 50 μm (middle and right). See also Table S1.

and a strong expression of type II collagen in the articular cartilage defects (Figures 6A and 6B), which differs from the observation that day-28 particles fail to produce mature cartilage in subcutaneous spaces. We speculate that the orthotopic environment might stimulate the maturation of day-28 particles. Side-to-side integration between the tissues formed by the transplanted cells and the rat articular cartilage was strongly achieved (Figure 6B). There were no signs of teratomas or other tumors in any of the four transplanted sites.

The human β-actin sequence was not amplified within 40 cycles in the real-time RT-PCR reactions among either the organs or lymph nodes of the SCID rats at 4 or 12 weeks after transplantation (Figure 6C). As with mice, our control experiment for rats show that this assay can be used to detect human sequences at a Ct value of 40 among samples containing 0.0003% human cells (Figure S6B). Together with the little or no expression of pluripotent markers observed in the hiPSC-derived chondrocytes on day 21 or later (Figures 3A and S4), these results suggest that hiPSC-derived cartilaginous particles obtained on day 28 neither form tumors nor ectopic tissue when implanted into defective articular cartilage.

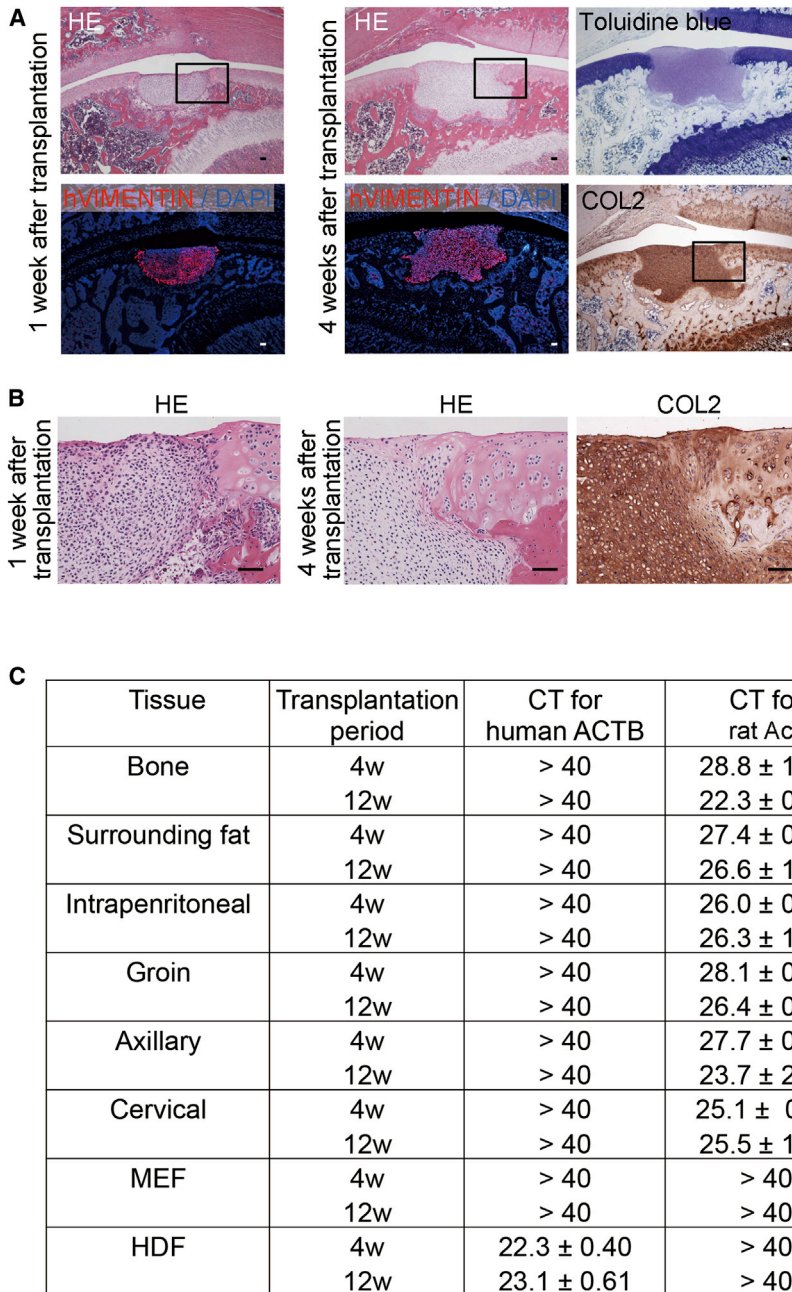### hiPSC-Derived Cartilaginous Particles Fixed Articular Defects in Mini-pigs

To examine whether hiPSC-derived cartilaginous particles can survive in the articular cartilage defects created in larger animals, we transplanted hiPSC-derived cartilaginous particles into defects created in the articular cartilage of three knees in mini-pigs weighing 27.0–30.5 kg and treated them with cyclosporine, an immunosuppressant. Trans-

planted particles survived in the defects of all three knees at 1 month after transplantation (Figure 7). Immunohistochemistry showed that cartilage filling the defects expressed human vimentin, confirming that progeny of the hiPSC-derived cartilaginous particles survived in the defects for at least 4 weeks. In addition, particles showed indications of integration with the host articular cartilage and with each other.

DISCUSSION

We herein developed an approach for differentiating hiPSCs toward chondrocytes capable of generating pure cartilage in vivo and fixing articular cartilage defects without tumor formation.

BMP2, TGF-β1, and GDF5 were required to obtain GFP-positive cells from *COL11A2-EGFP* hiPSC-derived mesendodermal cells. Plural receptors for BMPs (BMPRs) have been identified, and the affinity for these receptors has been shown to differ between BMPs and GDF5 (Nishitoh et al., 1996). In addition, BMPRIA and BMPRIB regulate distinct processes in the formation and differentiation of cartilage (Zou et al., 1997), and BMP and GDF family members have distinct functions in cartilage formation when overexpressed in transgenic mice (Tsumaki et al., 2002). Furthermore, both BMPRIA and BMPRIB are necessary for cartilage formation (Yoon et al., 2005). These findings are consistent with our results showing that both BMP2 and GDF5 are necessary for the differentiation of hiPSCs toward mature chondrocytes. It is also possible that BMP2, TGF-β1, and GDF5 were each required in our protocol, because we

Figure 6. Orthotopic Transplantation of hiPSC-Derived Cells into SCID Rats

hiPSC-derived cartilaginous particles obtained on day 28 were transplanted into defects created in the articular cartilage of the distal femurs of SCID rats. The transplanted sites (A and B) and various organs (C) were collected.

(A and B) Histological analysis of the transplanted sites at 1 and 4 weeks after transplantation. Semiserial sections were stained with H&E and toluidine blue and immunostained with anti-vimentin antibodies that recognize only human vimentin and anti-type II collagen antibodies. The blue color reflects DAPI. Magnified images of the boxed regions in (A) are shown in (B). Scale bars, 50 μm.

(C) RNAs were extracted from various organs at 4 and 12 weeks after transplantation and subjected to real-time RT-PCR to amplify human and rat β-actin mRNAs. n = 3 rats. The error bars denote the means ± SD. Bone, bone of the femoral diaphysis; Surrounding fat, fat tissue surrounding the transplanted sites; Intraperitoneal, intraperitoneal tissue; Groin, groin lymph nodes; Axillary, axillary lymph nodes; Cervical, cervical lymph nodes; MEF, murine embryonic fibroblasts; HDF, human dermal fibroblasts.

See also Figure S6 and Tables S1–S3.

Tissue	Transplantation period	CT for human ACTB	CT for rat Actb
Bone	4w	> 40	28.8 ± 1.21
	12w	> 40	22.3 ± 0.51
Surrounding fat	4w	> 40	27.4 ± 0.68
	12w	> 40	26.6 ± 1.02
Intraperitoneal	4w	> 40	26.0 ± 0.35
	12w	> 40	26.3 ± 1.49
Groin	4w	> 40	28.1 ± 0.24
	12w	> 40	26.4 ± 0.70
Axillary	4w	> 40	27.7 ± 0.59
	12w	> 40	23.7 ± 2.20
Cervical	4w	> 40	25.1 ± 0.97
	12w	> 40	25.5 ± 1.82
MEF	4w	> 40	> 40
	12w	> 40	> 40
HDF	4w	22.3 ± 0.40	> 40
	12w	23.1 ± 0.61	> 40

used iPSC-derived mesendodermal cells instead of more mature mesodermal tissues to induce chondrogenesis.

Articular cartilage is highly lubricious. Lubricin encoded by the PRG4 gene and glycosaminoglycans contribute to maintaining the low friction of cartilage and directly inhibit cell adhesion (Englert et al., 2005). Therefore, since the hiPSC-derived particles expressed *PRG4*, it is reasonable that the cartilaginous nodules formed in the hiPSC-derived cell culture were easily and reproducibly detached from the dishes and did not attach to the dishes again (Figure 3A).

In addition to the notion that three-dimensional cultures facilitate chondrocytic differentiation (Huey et al., 2012), the suspension culture appeared to contribute to removing non-chondrocytic cells and thus purification of the chondrocytic cells. Non-chondrocytic cells, once detached from the particles, may preferentially attach to the dish bottom (Figure S3). Furthermore, we employed chondrogenic culture conditions with a low concentration of FBS supplemented with a minimum of growth factors that are essential for chondrocyte survival. The non-chondrocytic
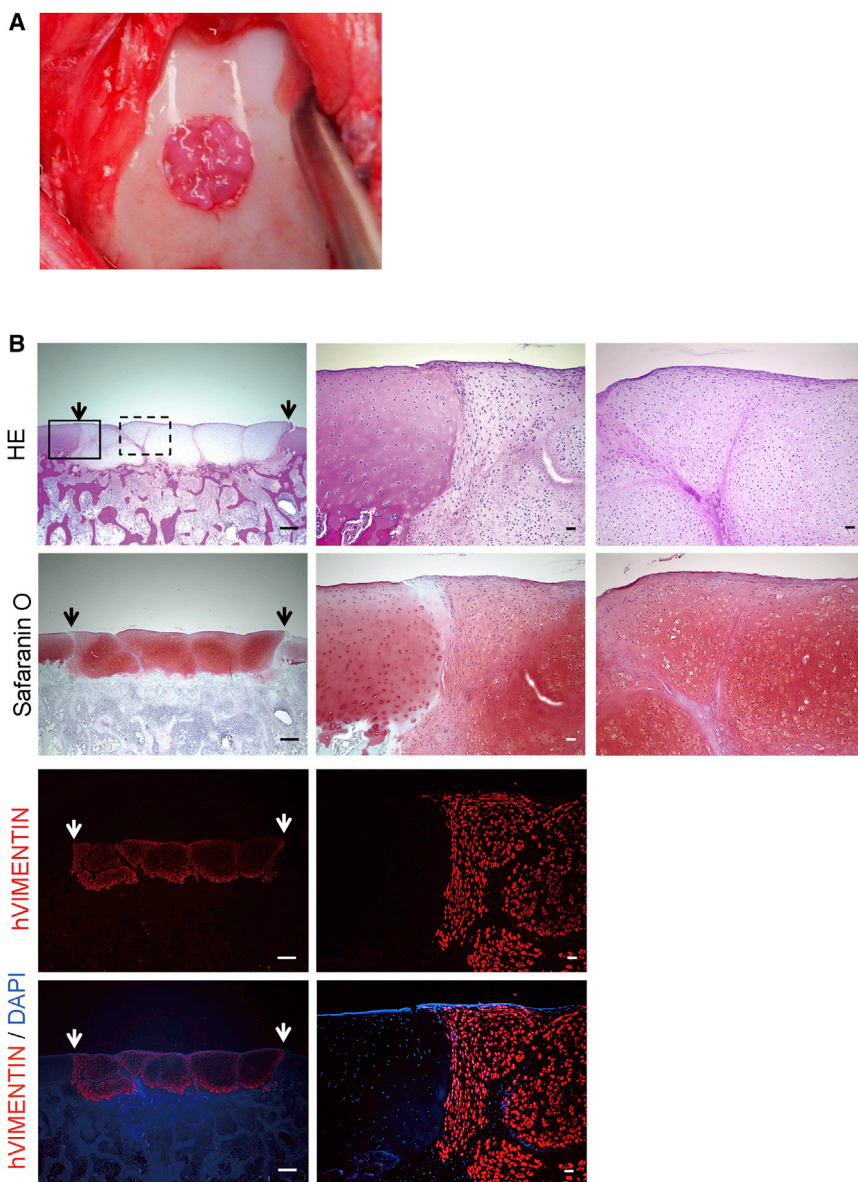
Figure 7. hiPSC-Derived Cartilaginous Particles Fixed Articular Defects in Mini-pigs

(A) hiPSC-derived cartilaginous particles (approximately ten) obtained on day 56 were transplanted into defects created in the articular cartilage of the distal femurs of mini-pigs and fixed with fibrin glue.

(B) Histological analysis of the transplanted sites at four weeks after transplantation. Semiserial sections were stained with H&E and safranin O-fast green-iron hematoxylin and immunostained with anti-vimentin antibodies that recognize only human vimentin. The blue color reflects DAPI. Magnified images of the solid boxed regions are shown in central panels. Magnified images of the dotted boxed regions are shown in right panels. Arrows indicate the boundary between native cartilage and transplanted cartilage. Scale bars, 500 μm (left) and 50 μm (right).

cells might die under these conditions (Figure 3B) and drop out from the particles. As a result of these purification steps, which include the transfer of non-adhesive chondrocyte clusters into a suspension culture, chondrocytic differentiation in a three-dimensional culture, the removal of non-chondrocytic cells from lubricious particles into the medium, and the selective death of non-chondrocytic cells, we succeeded in obtaining pure chondrocytes without the use of cell sorting. The result of this method was approximately 1.0×10^6 chondrocytes from $1.6 \pm 0.1 \times 10^5$ hiPSCs per 35-mm dish. Thus, our method is capable of producing sufficient numbers of cartilage particles to treat patients, as we can create 1.0×10^7 chondrocytes per ten 35-mm dishes, which is relatively easily to manage and is sufficient to cover a 10-cm^2 defect of articular cartilage in autologous chondrocyte implantations.

Articular cartilage remains permanent, and its bottom portion is slowly and continuously remodeled into underlying bone. In the present study, when hiPSC-derived cartilaginous particles were transplanted into the subcutaneous space of SCID mice, the cartilage remained intact for at least 1 year, while a portion of the chondrocytes slowly underwent hypertrophy and remodeling into bone-like tissue. This property of slow remodeling into bone may contribute to the vertical integration of neocartilage into underlying bone if transplanted into sites of defective articular cartilage. Treatment of the iPSC-derived particles with thyroid hormone induced the hypertrophy of chondrocytes

in vitro (unpublished data), suggesting the rate of hypertrophy is dependent on the protocol.

It has been difficult to achieve cartilage-to-cartilage integration because the cartilage ECM is anti-adhesive (van de Breevaart Bravenboer et al., 2004). Chondrocytes obtained from younger donors have been reported to achieve better side-to-side integration (Adkisson et al., 2010), raising the hypothesis that the use of immature chondrocytes results in better integration. The advantage of differentiating hiPSCs in a manner that mimics the developmental pathway includes the ability to generate chondrocytes with limited cellular senescence, which resembles chondrocytes from young individuals. In this study, the hiPSC-derived cartilaginous particles obtained on day 42 or longer displayed a mature cartilaginous ECM that was lubricious. On the other hand, the particles obtained on day 28 adhered to the shallow defects of SCID rat articular cartilage and were integrated into the adjacent native cartilage at 4 weeks after transplantation. We could not observe longer periods, because the remodeling of articular cartilage in rats was highly active, such that human chondrocytes present in the transplanted cartilage disappeared and were replaced with host rat chondrocytes within 8 to 12 weeks. This phenomenon was partly due to the small size of the defects in rats; the maximum appropriate defective size was 1 mm in diameter, since the width of the femoral groove in SCID rats was also ~1 mm. A similar phenomenon was also noted in rats treated with immunosuppressive drugs (Toh et al., 2010). The particles obtained on day 56 filled articular cartilage defects in mini-pigs and showed indications of integration with the native cartilage and each other at 4 weeks after transplantation, demonstrating that the particles have potential to fix cartilage defects even under heavy-weight-bearing conditions. The efficacy of transplanting hiPSC-derived chondrocytes into articular cartilage defects of mini-pigs for longer periods is for future study.

We used this differentiation method in a recently published paper for hiPSC disease modeling (Yamashita et al., 2014), in which analysis of FGFR3 skeletal dysplasia and drug screening were performed. We analyzed the safety and efficacy of cell transplantation into animals in the current study, demonstrating that our differentiation method is clinically relevant to cell transplantation therapy in regenerative medicine. In addition, we performed cellular analyses on the differentiation pathway using the GFP signal from the *COL11A-EGFP* line and on the appropriate time range and conditions required for in vitro maturation toward hyaline cartilage. These content would correspond to advancing the application of basic research from the laboratory to the clinic in regenerative medicine.

In summary, we herein developed a simple approach for differentiating hiPSCs into scaffoldless hyaline cartilage.

The use of iPSCs carries the risk of tumor formation in relation to the reprogramming method, a concern that does not exist for ESCs. However, we did not observe any formation of teratomas or tumors or of ectopic tissue in SCID mice and rats using our method when hiPSC-derived cartilage were transplanted either subcutaneously or orthotopically. Our results should contribute to an important step in translating the present procedure to clinical applications.

EXPERIMENTAL PROCEDURES

Ethics Statement
All experiments were approved by the institutional animal committee, institutional biosafety committee, and institutional review board of Kyoto University.

Chondrogenic Differentiation of hiPSCs
Integration-free hiPSC lines 409B2 and 604B1 (Okita et al., 2011) generated using episomal vectors were a gift from K. Okita and S. Yamanaka (Center for iPS Cell Research and Application [CiRA], Kyoto University, Kyoto, Japan). Episomal vectors bearing OCT3/4, SOX2, KLF4, LIN28, L-MYC, and p53 small hairpin RNA were transduced to generate hiPSCs. The episomal vectors were spontaneously lost during the establishment of the iPSC clones (Okita et al., 2011). HDF-11 and KF4009-1 were generated in our laboratory. Each hiPSC line was generated from the tissue of a different individual. The established hiPSCs were maintained on mitomycin-C-treated SNL (STO/Neo-resistant/LIF) cells in human ESC medium containing DMEM/F12 (Sigma), 20% KnockOut Serum Replacement (Invitrogen), 2 mM L-glutamine (Invitrogen), 1×10^{-4} M nonessential amino acids (Invitrogen), 1 mM Na pyruvate (Invitrogen), 1×10^{-4} M 2-mercaptoethanol (Invitrogen), 50 U and 50 mg/ml of penicillin and streptomycin, respectively (Invitrogen), and 4 ng/ml of bFGF (WAKO). The hiPSCs were transferred and then maintained in a feeder-free medium that included Essential 8 (Invitrogen) with 50 U/ml penicillin and 50 μg/ml streptomycin in 3.5-cm Matrigel-coated dishes. The hiPSCs formed high-density cell colonies that consisted of $1-2 \times 10^5$ cells 10–15 days after the start of maintenance under the feeder-free culture conditions. Subsequently, the hiPSCs were subjected to differentiation by changing the medium to a mesendodermal differentiation medium (DMEM/F12 with 10 ng/ml of Wnt3a [R&D Systems], 10 ng/ml of Activin A [R&D], 1% ITS; Invitrogen], 1% FBS, 50 U and 50 μg/ml of penicillin and streptomycin, respectively [Invitrogen]) (day 0). Three days later (day 3), the medium was changed to the basal medium (DMEM with 1% ITS, 1% FBS, 2 mM L-glutamine [Invitrogen], 1×10^{-4} M nonessential amino acids [Invitrogen], 1 mM Na pyruvate [Invitrogen], 50 U of penicillin, and 50 μg/ml of streptomycin) supplemented with one of five types of chondrogenic supplementation: A (50 μg/ml of ascorbic acid [Nacalai]), ABT (50 μg/ml of ascorbic acid, 10 ng/ml of BMP2 [Osteopharma], and 10 ng/ml of TGF-β1 [PeproTech]), ABTG (50 μg/ml of ascorbic acid, 10 ng/ml of BMP2, 10 ng/ml of TGF-β1, and 10 ng/ml of GDF5 [PTT]), ABG (50 μg/ml of ascorbic acid, 10 ng/ml of BMP2, and 10 ng/ml of GDF5), and ATG (50 μg/ml of ascorbic acid, 10 ng/ml of TGF-β1, and 10 ng/ml of GDF5). Fourteen days after

the start of the differentiation of the hiPSCs (day 14), the cartilaginous nodules were physically separated from the bottom of the dishes to form particles, which were then transferred to a suspension culture in 3.5-cm petri dishes. A total of 10 ng/ml of bFGF was added to the chondrogenic medium from day 3 to day 14 to increase proliferation. In some experiments, the medium was changed to conventional medium (DMEM with 10% FBS, 50 U and 50 μg/ml of penicillin and streptomycin, respectively) on day 42. The medium was changed every 2–7 days.

Generation of hiPSCs Bearing the *COL11A2-EGFP* Reporter Transgene

To construct the chondrocyte-specific reporter piggyBac vectors, the human sequences corresponding to the murine *Col11a2* promoter and enhancer were amplified via PCR. The murine *Col11a2* promoter/enhancer sequences of p742-gw-Int (pLI-gw, P1-20) were replaced by the human *COL11A2* promoter/enhancer sequences to prepare phProm-ENmcs(gw)-hInt (P16-22). phProm-ENmcs(gw)-hInt was recombined with pENTR1A-mcs/*Egfp-Ires-Puro* (P8-79) via an LR reaction (Invitrogen) to prepare phProm-gw(Egfp-IresPur)-hInt (P16-23). The hProm-gw(Egfp-IresPur)-hInt sequence was released from the plasmid backbone using PstI and FspI and inserted into the piggyBac vector PB-MCSII (P16-16), a gift from K. Woltjen (CiRA), to prepare PB-*hCOL11A2-EGFP* (PB-MCSII[hProm-gw(Egfp-IresPur)-hInt], P16-24). The PB-*hCOL11A2-EGFP* vector and transposase expression vector (PBaseII, P16-25), a gift from A. Hotta (CiRA), were introduced into the 409B2 hiPSCs (Okita et al., 2011) using nucleofection technology according to the manufacturer's instructions (Amaxa). Single-cell suspensions of the hiPSCs were plated onto 10-cm dishes. Approximately 10 days later, the colonies were mechanically picked up and hiPSC lines were established. The genomic integration of the PB-*hCOL11A2-EGFP* transgene was analyzed using genomic PCR. The primers used to amplify the transgene are listed in Table S3. Approximately 1.0×10^6 *hCOL11A2-EGFP* hiPSCs were implanted into the capsule of the testis in the SCID mice to form teratomas. Two months after implantation, the teratomas were dissected and subjected to immunohistochemical analysis of the EGFP expression.

Statistical Analysis

Data are shown as means and SDs. We used the Student's t test.

SUPPLEMENTAL INFORMATION

Supplemental Information includes Supplemental Experimental Procedures, six figures, and three tables and can be found with this article online at http://dx.doi.org/10.1016/j.stemcr.2015.01.016.

AUTHOR CONTRIBUTIONS

A.Y. was involved in most of the experiments. A.Y., M.M., and M.O. performed the differentiation of hiPSCs toward chondrocytes. M.M. and Y.Y. performed the immunohistological analyses. M.M. performed the DNA construction. Y.Y., T.K., S.K., S.M., and N.T. performed the mini-pig experiments. N.T. designed the study. A.Y. and N.T. wrote the paper.

REFERENCES

Adkisson, H.D., 4th, Martin, J.A., Amendola, R.L., Milliman, C., Mauch, K.A., Katwal, A.B., Seyedin, M., Amendola, A., Streeter, P.R., and Buckwalter, J.A. (2010). The potential of human allogeneic juvenile chondrocytes for restoration of articular cartilage. Am. J. Sports Med. *38*, 1324–1333.

Bai, H.Y., Chen, G.A., Mao, G.H., Song, T.R., and Wang, Y.X. (2010). Three step derivation of cartilage like tissue from human embryonic stem cells by 2D-3D sequential culture in vitro and further implantation in vivo on alginate/PLGA scaffolds. J. Biomed. Mater. Res. A *94*, 539–546.

Barberi, T., Willis, L.M., Socci, N.D., and Studer, L. (2005). Derivation of multipotent mesenchymal precursors from human embryonic stem cells. PLoS Med. *2*, e161.

Bigdeli, N., Karlsson, C., Strehl, R., Concaro, S., Hyllner, J., and Lindahl, A. (2009). Coculture of human embryonic stem cells and human articular chondrocytes results in significantly altered phenotype and improved chondrogenic differentiation. Stem Cells *27*, 1812–1821.

Cheng, A., Kapacee, Z., Peng, J., Lu, S., Lucas, R.J., Hardingham, T.E., and Kimber, S.J. (2014). Cartilage repair using human embryonic stem cell-derived chondroprogenitors. Stem Cells Transl. Med. *3*, 1287–1294.

Englert, C., McGowan, K.B., Klein, T.J., Giurea, A., Schumacher, B.L., and Sah, R.L. (2005). Inhibition of integrative cartilage repair by proteoglycan 4 in synovial fluid. Arthritis Rheum. *52*, 1091–1099.

Hiramatsu, K., Sasagawa, S., Outani, H., Nakagawa, K., Yoshikawa, H., and Tsumaki, N. (2011). Generation of hyaline cartilaginous tissue from mouse adult dermal fibroblast culture by defined factors. J. Clin. Invest. *121*, 640–657.

Huey, D.J., Hu, J.C., and Athanasiou, K.A. (2012). Unlike bone, cartilage regeneration remains elusive. Science *338*, 917–921.

Hwang, N.S., Varghese, S., and Elisseeff, J. (2008). Derivation of chondrogenically-committed cells from human embryonic cells for cartilage tissue regeneration. PLoS ONE *3*, e2498.

Ko, J.Y., Kim, K.I., Park, S., and Im, G.I. (2014). In vitro chondrogenesis and in vivo repair of osteochondral defect with human induced pluripotent stem cells. Biomaterials 35, 3571–3581.

Koay, E.J., Hoben, G.M., and Athanasiou, K.A. (2007). Tissue engineering with chondrogenically differentiated human embryonic stem cells. Stem Cells 25, 2183–2190.

Koyama, N., Miura, M., Nakao, K., Kondo, E., Fujii, T., Taura, D., Kanamoto, N., Sone, M., Yasoda, A., Arai, H., et al. (2013). Human induced pluripotent stem cells differentiated into chondrogenic lineage via generation of mesenchymal progenitor cells. Stem Cells Dev. 22, 102–113.

Medvedev, S.P., Grigor'eva, E.V., Shevchenko, A.I., Malakhova, A.A., Dementyeva, E.V., Shilov, A.A., Pokushalov, E.A., Zaidman, A.M., Aleksandrova, M.A., Plotnikov, E.Y., et al. (2011). Human induced pluripotent stem cells derived from fetal neural stem cells successfully undergo directed differentiation into cartilage. Stem Cells Dev. 20, 1099–1112.

Mithoefer, K., McAdams, T., Williams, R.J., Kreuz, P.C., and Mandelbaum, B.R. (2009). Clinical efficacy of the microfracture technique for articular cartilage repair in the knee: an evidence-based systematic analysis. Am. J. Sports Med. 37, 2053–2063.

Nakagawa, T., Lee, S.Y., and Reddi, A.H. (2009). Induction of chondrogenesis from human embryonic stem cells without embryoid body formation by bone morphogenetic protein 7 and transforming growth factor beta1. Arthritis Rheum. 60, 3686–3692.

Nishitoh, H., Ichijo, H., Kimura, M., Matsumoto, T., Makishima, F., Yamaguchi, A., Yamashita, H., Enomoto, S., and Miyazono, K. (1996). Identification of type I and type II serine/threonine kinase receptors for growth/differentiation factor-5. J. Biol. Chem. 271, 21345–21352.

Okita, K., Ichisaka, T., and Yamanaka, S. (2007). Generation of germline-competent induced pluripotent stem cells. Nature 448, 313–317.

Okita, K., Matsumura, Y., Sato, Y., Okada, A., Morizane, A., Okamoto, S., Hong, H., Nakagawa, M., Tanabe, K., Tezuka, K., et al. (2011). A more efficient method to generate integration-free human iPS cells. Nat. Methods 8, 409–412.

Oldershaw, R.A., Baxter, M.A., Lowe, E.T., Bates, N., Grady, L.M., Soncin, F., Brison, D.R., Hardingham, T.E., and Kimber, S.J. (2010). Directed differentiation of human embryonic stem cells toward chondrocytes. Nat. Biotechnol. 28, 1187–1194.

Roberts, S., Menage, J., Sandell, L.J., Evans, E.H., and Richardson, J.B. (2009). Immunohistochemical study of collagen types I and II and procollagen IIA in human cartilage repair tissue following autologous chondrocyte implantation. Knee 16, 398–404.

Steck, E., Fischer, J., Lorenz, H., Gotterbarm, T., Jung, M., and Richter, W. (2009). Mesenchymal stem cell differentiation in an experimental cartilage defect: restriction of hypertrophy to bone-close neocartilage. Stem Cells Dev. 18, 969–978.

Taiani, J.T., Krawetz, R.J., Zur Nieden, N.I., Elizabeth Wu, Y., Kallos, M.S., Matyas, J.R., and Rancourt, D.E. (2010). Reduced differentiation efficiency of murine embryonic stem cells in stirred suspension bioreactors. Stem Cells Dev. 19, 989–998.

Toh, W.S., Lee, E.H., Guo, X.M., Chan, J.K., Yeow, C.H., Choo, A.B., and Cao, T. (2010). Cartilage repair using hyaluronan hydrogel-encapsulated human embryonic stem cell-derived chondrogenic cells. Biomaterials 31, 6968–6980.

Tsumaki, N., Kimura, T., Matsui, Y., Nakata, K., and Ochi, T. (1996). Separable cis-regulatory elements that contribute to tissue- and site-specific alpha 2(XI) collagen gene expression in the embryonic mouse cartilage. J. Cell Biol. 134, 1573–1582.

Tsumaki, N., Nakase, T., Miyaji, T., Kakiuchi, M., Kimura, T., Ochi, T., and Yoshikawa, H. (2002). Bone morphogenetic protein signals are required for cartilage formation and differently regulate joint development during skeletogenesis. J. Bone Miner. Res. 17, 898–906.

Umeda, K., Zhao, J., Simmons, P., Stanley, E., Elefanty, A., and Nakayama, N. (2012). Human chondrogenic paraxial mesoderm, directed specification and prospective isolation from pluripotent stem cells. Sci. Rep. 2, 455.

van de Breevaart Bravenboer, J., In der Maur, C.D., Bos, P.K., Feenstra, L., Verhaar, J.A., Weinans, H., and van Osch, G.J. (2004). Improved cartilage integration and interfacial strength after enzymatic treatment in a cartilage transplantation model. Arthritis Res. Ther. 6, R469–R476.

Vats, A., Bielby, R.C., Tolley, N., Dickinson, S.C., Boccaccini, A.R., Hollander, A.P., Bishop, A.E., and Polak, J.M. (2006). Chondrogenic differentiation of human embryonic stem cells: the effect of the micro-environment. Tissue Eng. 12, 1687–1697.

Wakitani, S., Takaoka, K., Hattori, T., Miyazawa, N., Iwanaga, T., Takeda, S., Watanabe, T.K., and Tanigami, A. (2003). Embryonic stem cells injected into the mouse knee joint form teratomas and subsequently destroy the joint. Rheumatology (Oxford) 42, 162–165.

Wei, Y., Zeng, W., Wan, R., Wang, J., Zhou, Q., Qiu, S., and Singh, S.R. (2012). Chondrogenic differentiation of induced pluripotent stem cells from osteoarthritic chondrocytes in alginate matrix. Eur. Cell. Mater. 23, 1–12.

Yamashita, A., Liu, S., Woltjen, K., Thomas, B., Meng, G., Hotta, A., Takahashi, K., Ellis, J., Yamanaka, S., and Rancourt, D.E. (2013). Cartilage tissue engineering identifies abnormal human induced pluripotent stem cells. Sci. Rep. 3, 1978.

Yamashita, A., Morioka, M., Kishi, H., Kimura, T., Yahara, Y., Okada, M., Fujita, K., Sawai, H., Ikegawa, S., and Tsumaki, N. (2014). Statin treatment rescues FGFR3 skeletal dysplasia phenotypes. Nature 513, 507–511.

Yoon, B.S., Ovchinnikov, D.A., Yoshii, I., Mishina, Y., Behringer, R.R., and Lyons, K.M. (2005). Bmpr1a and Bmpr1b have overlapping functions and are essential for chondrogenesis in vivo. Proc. Natl. Acad. Sci. USA 102, 5062–5067.

Zhao, J., Li, S., Trilok, S., Tanaka, M., Jokubaitis-Jameson, V., Wang, B., Niwa, H., and Nakayama, N. (2014). Small molecule-directed specification of sclerotome-like chondroprogenitors and induction of a somitic chondrogenesis program from embryonic stem cells. Development 141, 3848–3858.

Zou, H., Wieser, R., Massague, J., and Niswander, L. (1997). Distinct roles of type I bone morphogenetic protein receptors in the formation and differentiation of cartilage. Genes Dev. 11, 2191–2203.